

**Electronic supplementary information (ESI)**

**Morphology tailoring and improved electrochemical performance of hexagonal boron nitride (h-BN) for symmetric supercapacitor applications**

Madhav Dobhal<sup>a</sup>, Aditya Sharma<sup>\*a</sup>, Bhavi Agrawal<sup>a</sup>, Mayora Varshney<sup>b</sup>, Hyun-Joon Shin<sup>c#</sup>, Ranjeet Kumar Brajpuriya<sup>a</sup>, and Shalendra Kumar<sup>a</sup>

<sup>a</sup>Department of Physics, SOAE, University of Petroleum and Energy Studies (UPES), Dehradun, Uttarakhand, 248007, India.

<sup>b</sup>Department of Applied and Life Sciences, & Division of Research & Innovation, Uttaranchal University, Dehradun, Uttarakhand 248007, India.

<sup>c</sup>Department of Physics, Chungbuk National University, Cheongju-28644, South Korea.

[\\*adityaiuac@gmail.com](mailto:adityaiuac@gmail.com), [#shin@chungbuk.ac.kr](mailto:shin@chungbuk.ac.kr)

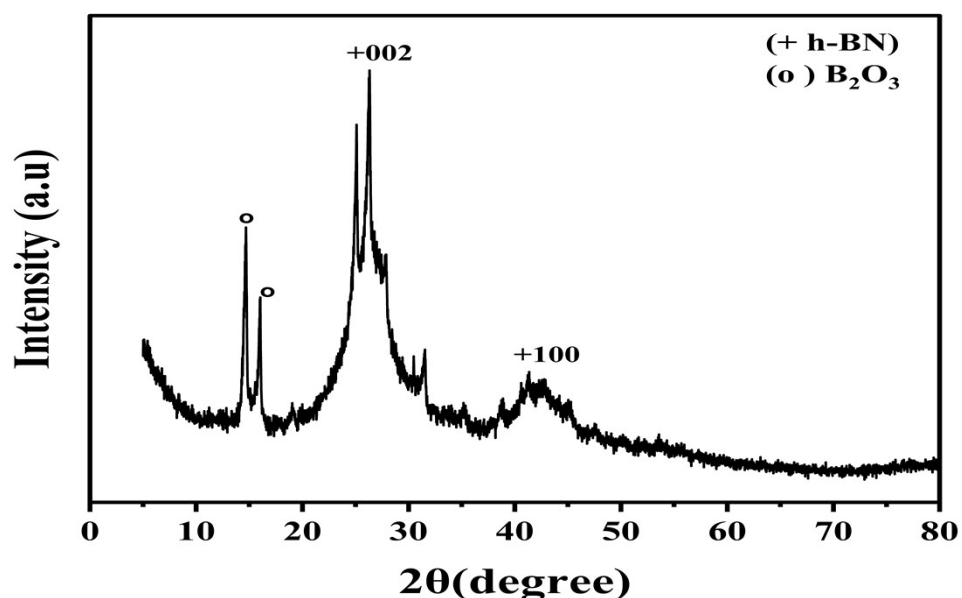


**Figure S1.** XRD pattern showing mixed-phase formation, where reflections of h-BN are accompanied by a distinct peak near  $\sim 15^\circ$ , corresponding to the B<sub>2</sub>O<sub>3</sub> phase.

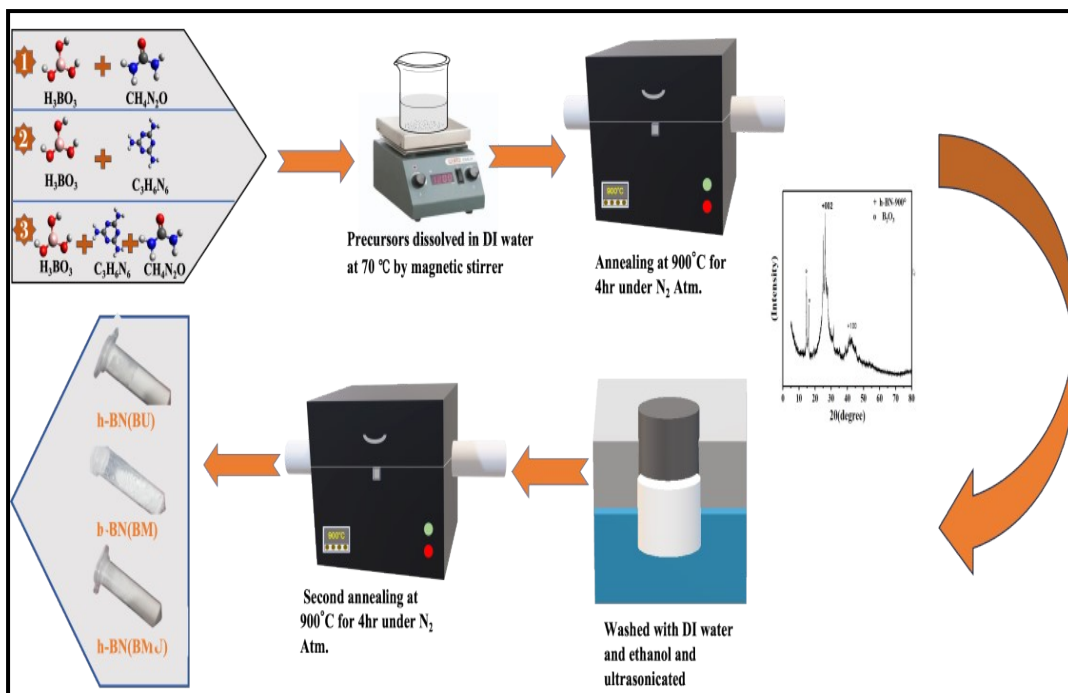


**Figure S2.** Synthesis process of h-BN using different precursor combinations: boric acid-urea (h-BN(BU)), boric acid- melamine (h-BN(BM)), boric acid-urea-melamine (h-BN(BMU)).

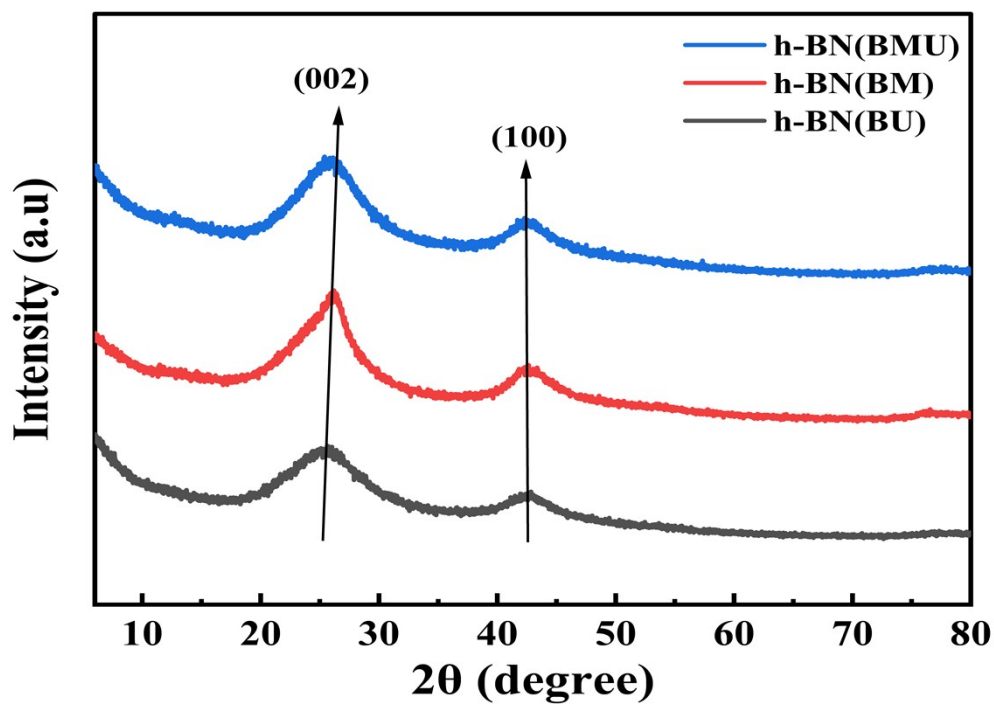


**Figure S3.** XRD patterns of h-BN(BU), h-BN(BM), and h-BN(BMU) samples prepared via different precursor routes, showing the characteristic (002) and (100) reflections of hexagonal boron nitride.

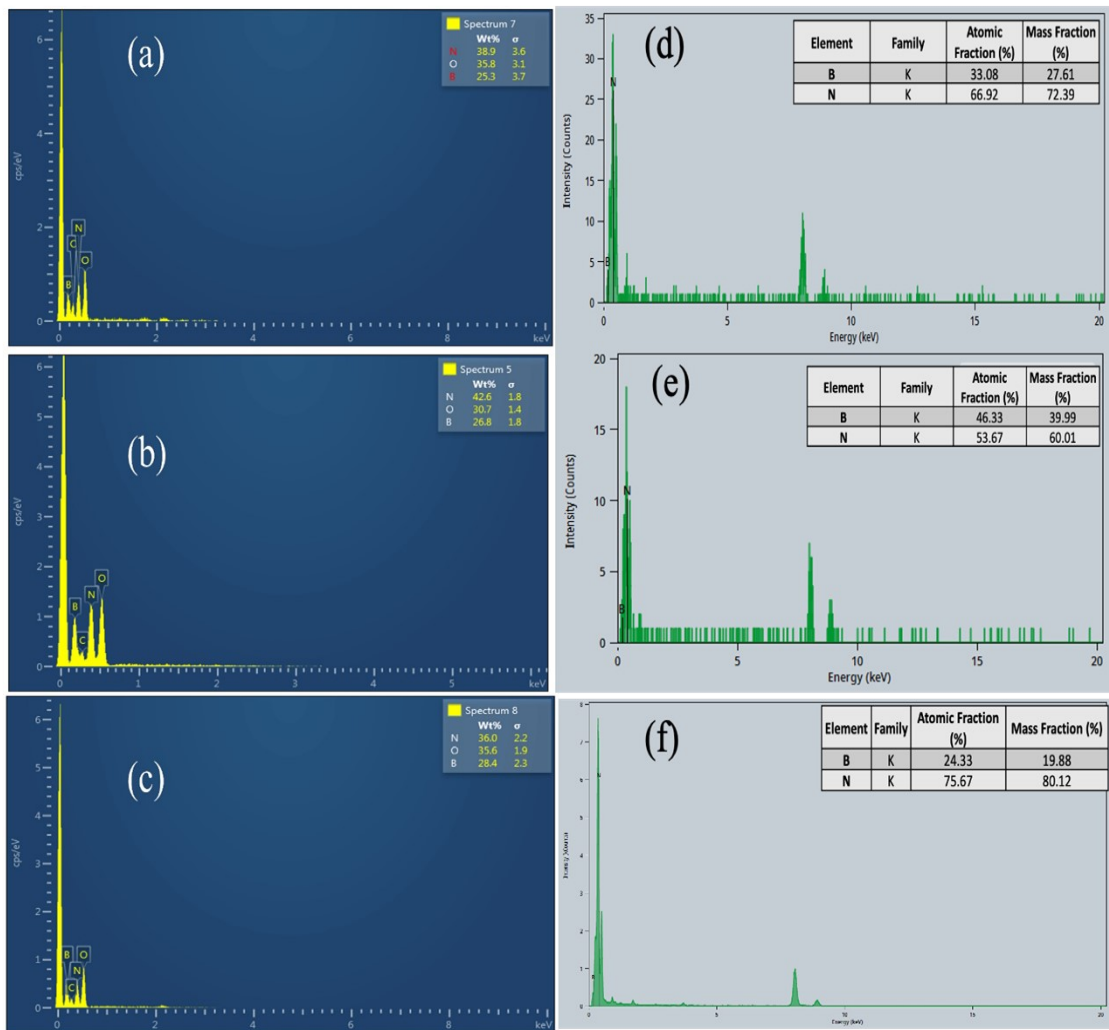


**Figure S4.** EDS from FE-SEM of (a) h-BN(BU), (b) h-BN(BM), (c) h-BN(BMU). And from TEM (d) h-BN(BU), (e) h-BN(BM), (f) h-BN(BMU).

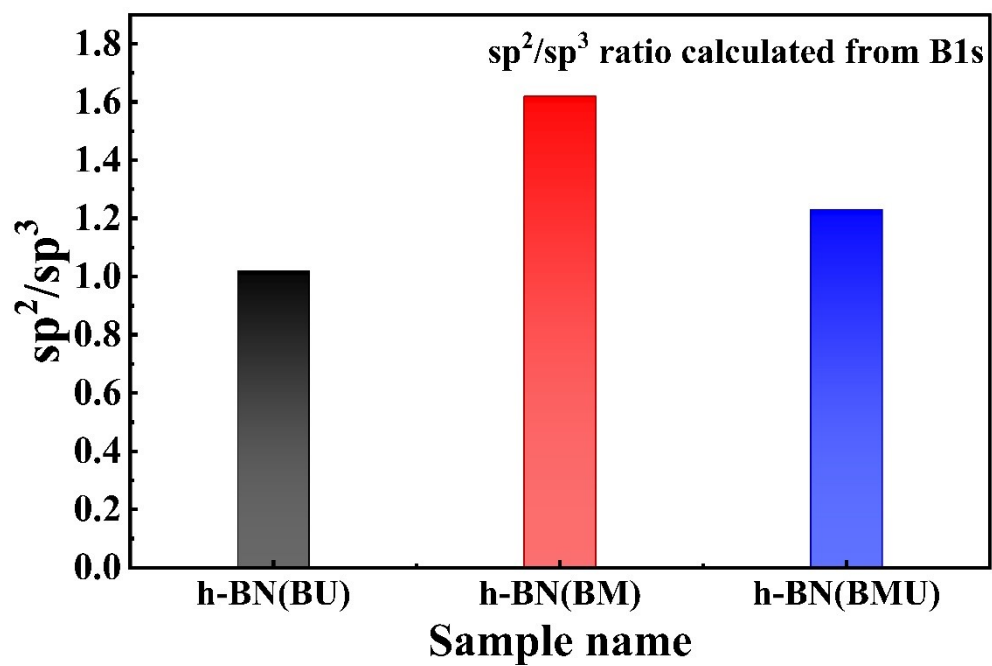


**Figure S5.** sp<sup>2</sup>/sp<sup>3</sup> ratios of *h*-BN(BU), *h*-BN(BM), and *h*-BN(BMU), evaluated from B1s XPS spectra.

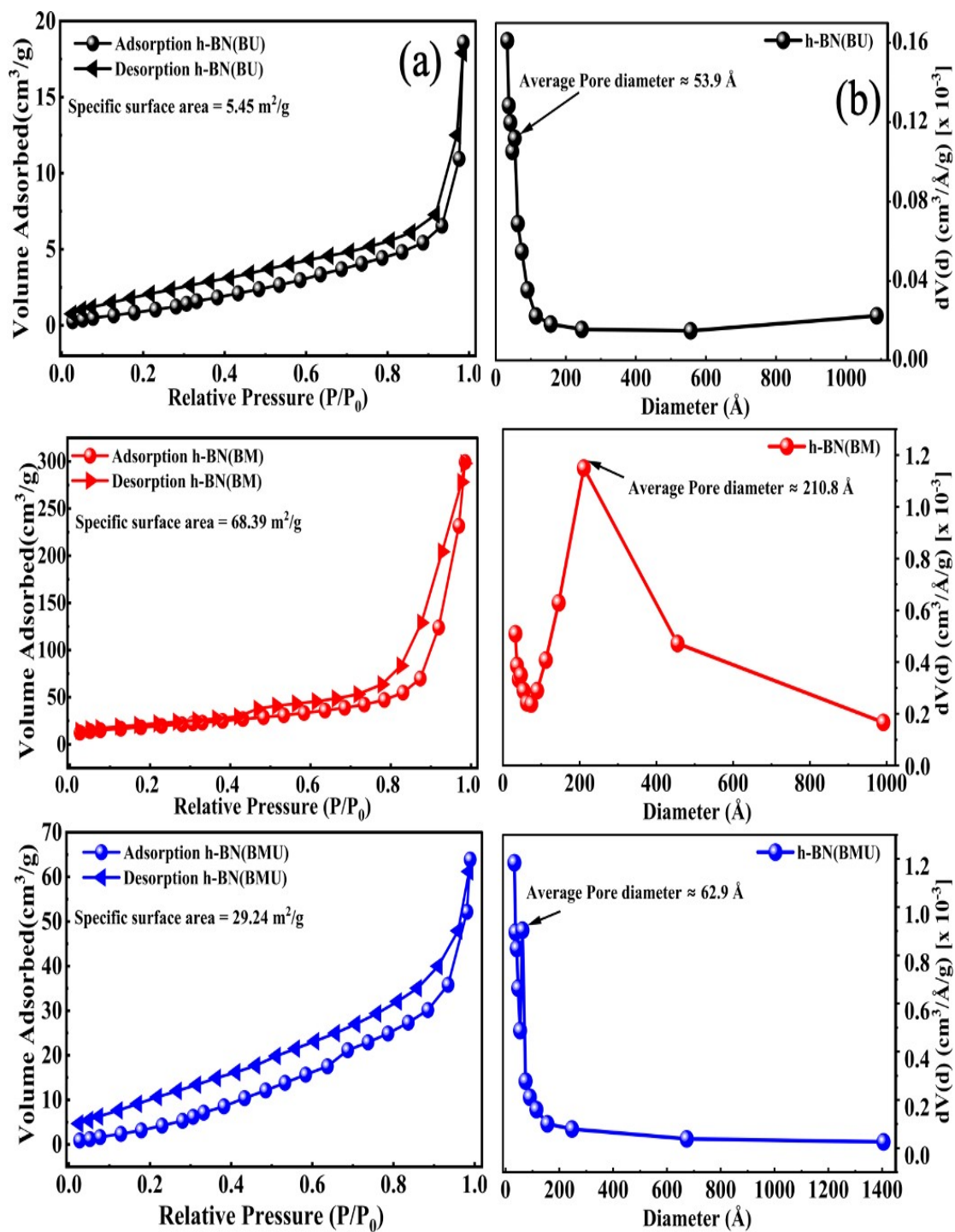


**Figure S6.** BET analysis of nitrogen adsorption-desorption isotherms and pore size distribution curves of *h*-BN(BU), *h*-BN(BM), and *h*-BN (BMU) samples.

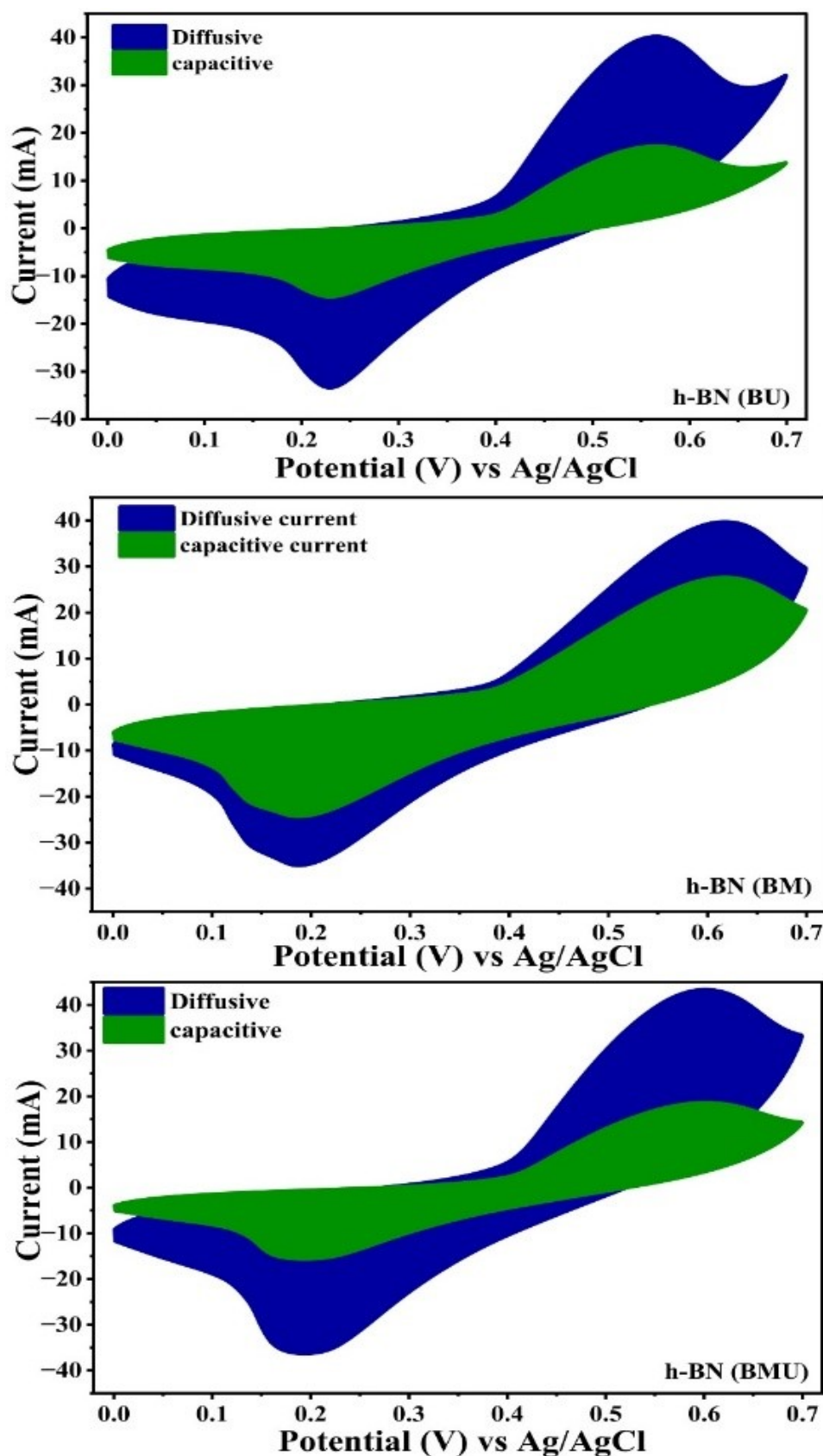


**Figure S7.** Comparison of capacitive and diffusive contributions in CV data (taken at a scan rate of 100 mV/s) of *h*-BN(BU), *h*-BN(BM), and *h*-BN(BMU) samples.

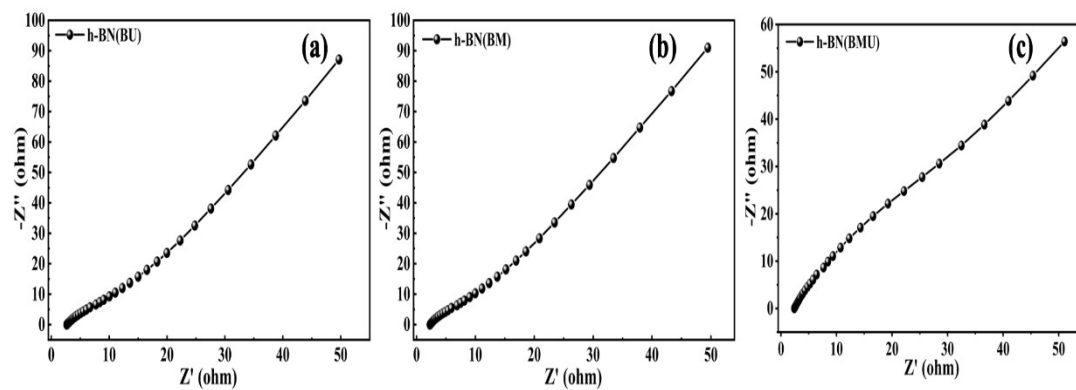


**Figure S8.** Nyquist plots of (a) h-BN(BU), (b) h-BN(BM), (c) h-BN(BMU).

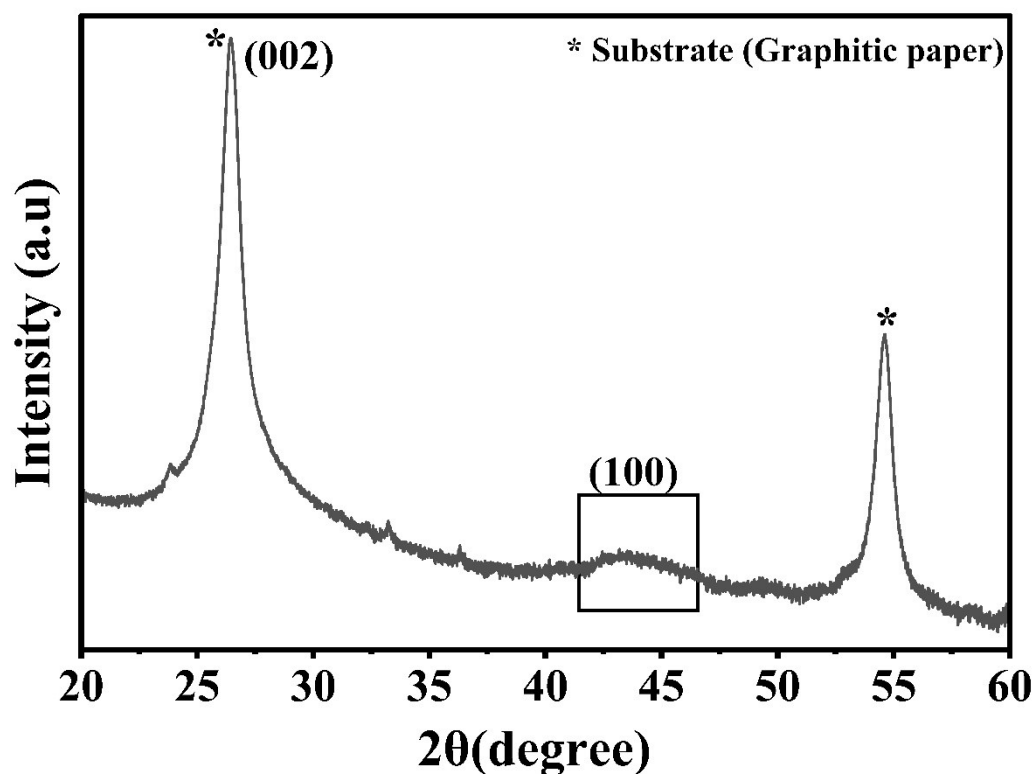


**Figure S9** XRD patterns collected after 10,000 charging-discharging cycles, of the h-BN (BM) electrodes prepared on Graphitic paper.

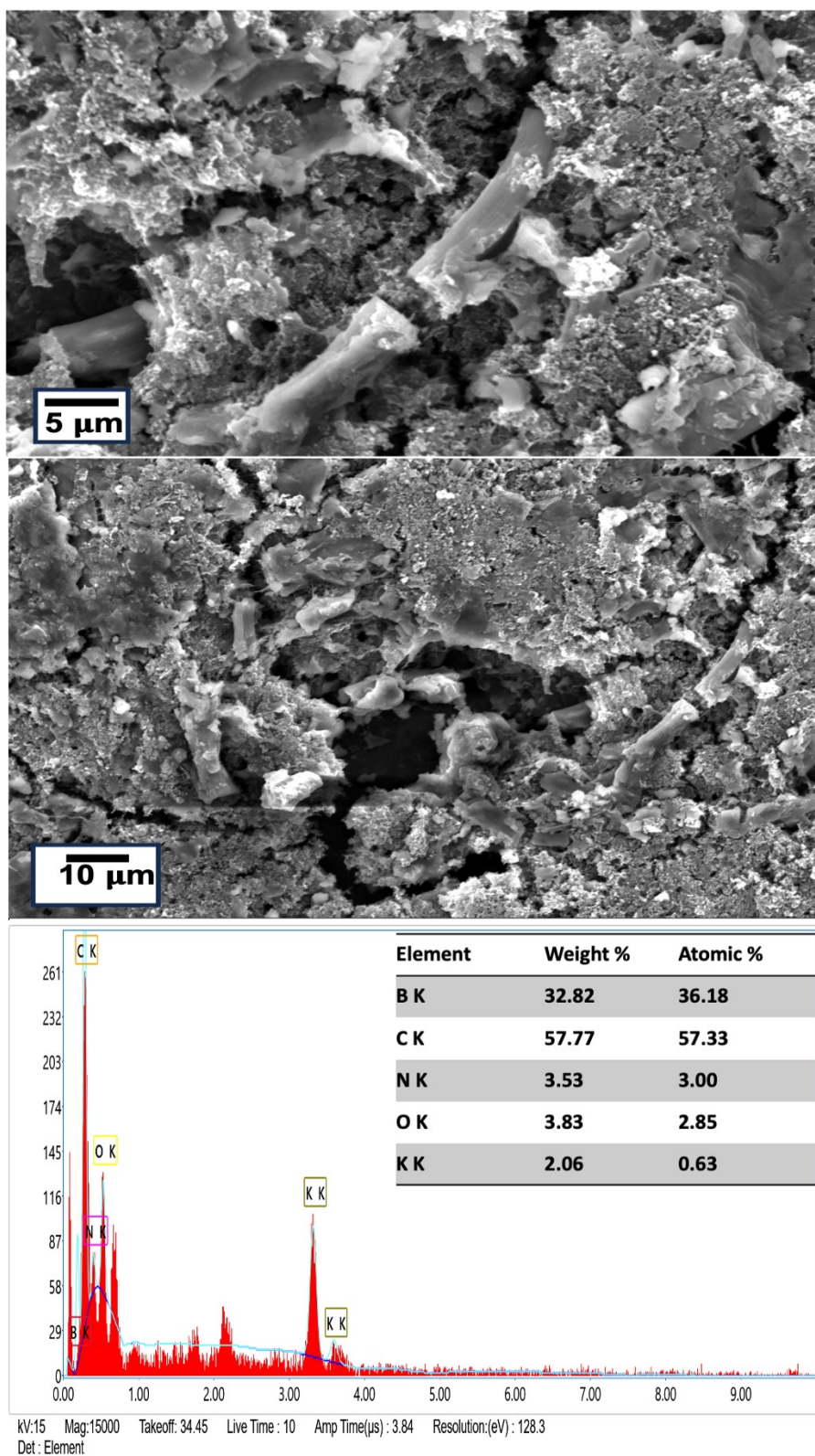


**Figure.S10** SEM images and EDS, collected after 10,000 charging-discharging cycles of the h-BN (BM) electrode prepared on Graphitic paper. Higher magnification SEM images show the existence of rod-like morphology. The EDS shows K-related peaks due to the residual KOH present in the electrode.

**Table S1.** Structural parameters of h-BN samples synthesized via different precursor combinations, including lattice constants, interplanar spacing ( $d_{002}$ ), average crystalline size (D), cell volume and  $\chi^2$  values derived from XRD.

Sample name	Lattice constant a=b (Å)	Lattice constant c (Å)	Interplanar spacing $d_{(002)}$ (Å)	Crystallite size D (nm)	Cell volume Å <sup>3</sup>	$\chi^2$	Rp	Rwp	Rexp
<i>h</i> -BN(BU)	2.556	7.032	3.51	1.3	39.77	2.27	4.23	5.57	3.70
<i>h</i> -BN(BM)	2.455	6.810	3.40	1.4	35.56	2.90	5.16	6.38	3.74
<i>h</i> -BN(BMU)	2.541	6.920	3.46	1.5	38.72	2.06	4.25	5.42	3.77

**Table S2.** XPS deconvolution results of the B 1s and N 1s core-level spectra for h-BN(BU), h-BN(BM), and h-BN(BMU) samples, showing binding energies and relative percentage contributions of B–N, B–O, N–B, and N–H bonding states.

Sample Name	Region	Labelling	Binding Energy (eV)	% contribution	(sp <sup>2</sup> /sp <sup>3</sup> ) ratio
<i>h</i> -BN(BU)	B1s	B-N	190.83	50.40 %	1.01
		B-O	192.42	49.60%	
	N1s	N-B	398.47	81.04%	1.62
		N-H	400.30	18.96%	
<i>h</i> -BN(BM)	B1s	B-N	190.65	61.90%	1.62
		B-O	192.32	38.10%	
	N1s	N-B	398.30	87.93%	1.23
		N-H	400.20	12.14%	
<i>h</i> -BN(BMU)	B1s	B-N	190.58	55.32%	1.23
		B-O	192.43	44.68%	
	N1s	N-B	398.04	86.30%	1.23
		N-H	400.02	13.70%	

**Table S3.** Specific capacitance of h-BN(BU), h-BN(BM) and h-BN(BMU) calculated from CV at different scan rates in 1 M KOH electrolyte.

Scan Rate (mV/s)	C <sub>sp</sub> h-BN(BU) (F/g)	C <sub>sp</sub> h-BN(BM) ( F/g)	C <sub>sp</sub> h-BN(BMU) (F/g)
2	455.0	516.8	493.3
5	415.3	461.9	445.2
10	369.9	415.5	390.5
25	282.8	335.4	303.2
50	212.5	264.2	232.4
75	174.2	224.7	195.0
100	152.4	196.2	168.9

**Table S4.** Specific capacitance of h-BN(BU), h-BN(BM) and h-BN(BMU) calculated from GCD at different current densities in 1 M KOH electrolyte.

Current Density (A/g)	C <sub>sp</sub> h-BN(BU) (F/g)	C <sub>sp</sub> h-BN(BM) (F/g)	C <sub>sp</sub> h-BN(BMU) (F/g)
1	429.5	479.2	431.3
2	390.3	449.6	384.6
3	359.1	424.3	353.8
4	332.9	402.4	326.4
5	309.7	382.3	301.7
10	227.8	306.8	218.8